

# Study of a Laser Packaging Technique Simulated with ANSYS and VirtualLab Fusion Software

P. Ribes-Pleguezuelo<sup>1,2,\*</sup>, S. Zhang<sup>2</sup>, E. Beckert<sup>1</sup>, R. Eberhardt<sup>1</sup>, F. Wyrowski<sup>2</sup>, A. Tünnermann<sup>1,2</sup>

<sup>1</sup>Fraunhofer Institute for Applied Optics and Precision Engineering IOF, Albert-Einstein-Str. 7, 07745 Jena, Germany

<sup>2</sup>Institute of Applied Physics, Abbe Center of Photonics, Friedrich Schiller University Jena, Max-Wien-Platz 1, 07743 Jena, Germany

\*[pol.ribes@iof.fraunhofer.de](mailto:pol.ribes@iof.fraunhofer.de)

**Abstract:** Mechanico-optical simulations performed with ANSYS and VirtualLab Fusion software to analyze stress-induced birefringence for the packaging of a laser ignition device by a low-stress soldering technique showed almost no influence on the laser output beam.

**OCIS codes:** (140.0140) Lasers and laser optics; (220.0220) Optical design and fabrication; (260.1440) Birefringence.

## 1. Introduction

Compact and miniaturized laser devices capable of operation under extreme conditions; as laser ignition devices that have to perform under high ambient temperature and vibrations, present a challenging goal for laser manufacturers. Such devices require high output power with a high thermal, wavelength and beam stability by minimizing the size and weight. To accomplish this, new assembling techniques have to be assessed.

We present a low-stress and localized soldering technique able to join laser crystals with their housing packaging materials via soft soldering alloys. Solderjet bumping technique uses spherical soft solder alloy preforms with a diameter range between 40 to 760  $\mu\text{m}$ . In preference to joining laser crystals to metallic housings by a soldering technique, solderjet bumping technique requires components with a wettable metallic surface on the components to be bonded. This metallic interface could be applied by physical vapor deposition (PVD) [1]. Although this technique has been used already to assemble laser devices [2], the laser packaging designs have to be studied in terms of stress-induced birefringence to prevent possible laser resonator misbehavior, which could compromise laser quality and power drop off.

## 2. Laser resonator and housing design

For our case of study, we have chosen a plano-plano monolithic laser cavity (Fig.1.) represented by a Cr:YAG crystal, based on the geometry published results of G. Salamu et. al. [3]. The selected soft solder alloy used to join the laser components to a stainless steel housing was SnAgCu (SAC).

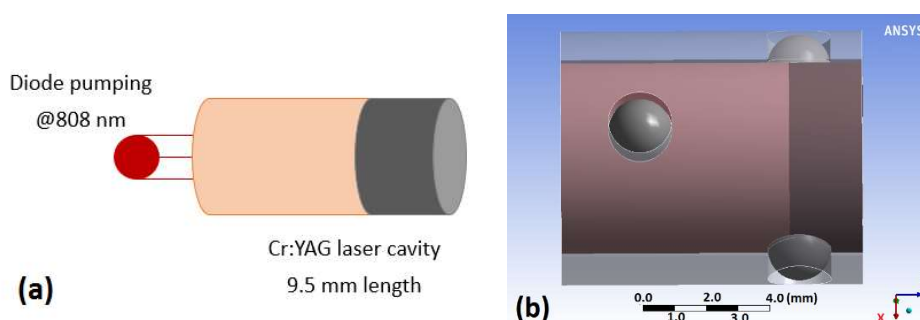


Fig. 1. (a) Schematic of the studied diode-pumped solid-state laser cavity. A pumping diode at 808 nm, and the plano-plano laser cavity represented by a monolithic 9.5 mm Cr:YAG. (b) Stainless steel housing cylinder assembled to a Cr:YAG crystal by four 760  $\mu\text{m}$  diameter SAC305 solder droplets alloy (bumps are being magnified at the image).

The simulations were performed first with a Finite Element Method (FEM) using ANSYS 17.0 software to replicate the crystal packaging procedures and calculate the induced stresses. Then, the calculated stress-induced

birefringence was converted into the dielectric matrix thanks to each component's piezo-optic tensor, to be finally imported to VirtualLab Fusion software to study the packaged components lasing capabilities.

### 3. Stress-induced birefringence analysis methodology

The soldering packaging mechanical process has been simulated with ANSYS Design Modeler. A transient thermal simulation using the alloy enthalpy (approximate melting temperature 217 °C) has been used to analyze the alloy solidification (thermal range from 230 °C to 22 °C) onto the laser crystal. With a post processing analysis, we extracted the vector principal stresses along the optical beam path inside the laser components in order to study the component's birefringence and possible lasing misbehavior.

Later, the mechanical induced stress onto the crystal has been analyzed following the produced changes on the crystal indicatrix (3D representation of crystal refractive indexes)  $B_{ij}$ ,

$$B_{ij} = B_{0,ij} + \Delta B_{ij} \quad (1)$$

the second-rank tensor  $B_{0,ij}$  represents the free-of-stress indicatrix tensor, and  $\Delta B_{ij}$  represents the indicatrix changes produced due to induced stress, which can also be expressed as,

$$\Delta B_{ij} = \pi_{ijkl} \sigma_{kl} \quad (2)$$

where second-rank tensor  $\sigma_{kl}$  represents the induced vector principal stress, and  $\pi_{ijkl}$  is the fourth-rank piezo-optic constants tensor described for each material. With both Eq. (1) and (2), we can calculate the indicatrix tensor  $B_{ij}$  when certain stress  $\sigma_{kl}$  is present. Then, the dielectric constant tensor  $\epsilon_{ij}$  can be calculated using the following relation:

$$[\epsilon_{ij}] = [B_{ij}]^{-1} \quad (3)$$

the resulting permeability matrix  $\epsilon_{ij}$  is to be used for the subsequent optical simulation on the crystals by using VirtualLab Fusion software [4].

### 4. Results

The mechanical transient thermal analysis simulated with ANSYS 17.0 were coupled sub-step by sub-step to a static structural analysis where the crystal internal stresses were calculated.

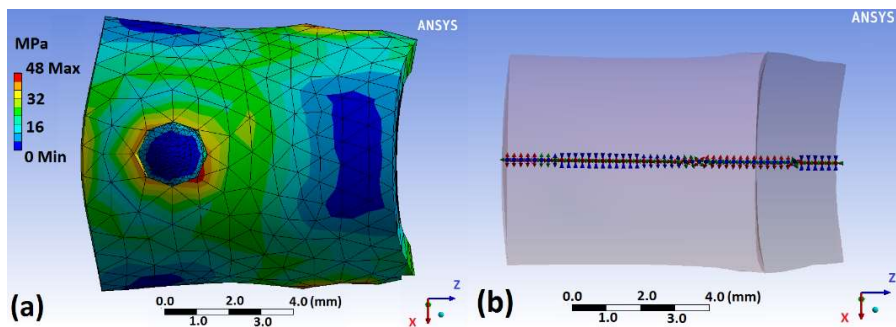


Fig. 2. (a) Magnified Von-Mises stress calculated in MPa. (b) Vector principal stresses calculated along the laser beam propagation direction in MPa (maximum, middle and minimum principal stresses in red, green and blue; respectively).

Then, the vector principal stresses in MPa were extracted following a laser beam propagation path and transformed into changes of the components indicatrix matrix thanks to the piezo-optic tensors calculated in the laboratory system [5]. Later, the stress induced effects were analyzed with VirtualLab Fusion software thanks to the calculated crystal dielectric permeability under induced stress. Different stress cases were evaluated as described in the Table 1.

Table 1. Studied laser resonator cavity produced beams and stress crystal conditions.

| Laser cavity beam  | Crystal condition (YAG/BBO/Fused quartz)  |
|--|---|
| 1. Gaussian @1064 nm from YAG emission, 50 $\mu$ m waist radius, $E_y$ -polarization | a. Ideal case: without stress<br>b. Real case: with actual applied stress<br>c. Comparing case: with increased stress (10x) by design |

The resulting YAG crystal  $E_y$ -polarized input and output beam at 1064 nm under the three different conditions can be seen in Fig. 3.

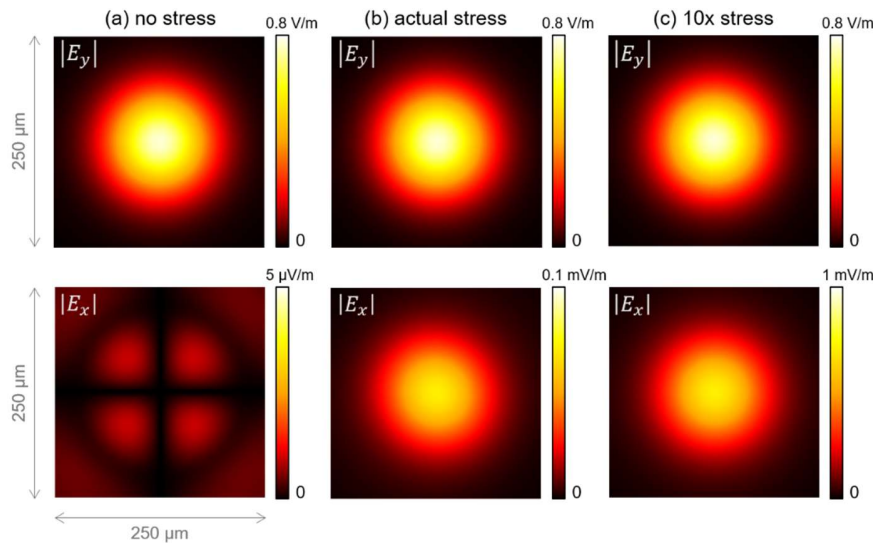


Fig. 3. Amplitude of the transmitted field behind the YAG crystal, with  $E_y$ -polarized Gaussian at 1064 nm as the input. Column (a) ideal case without stress; column (b): with actual solderjet bumping packaging induced stress; column (c): with 10× increased stress. Upper row corresponds to the  $E_y$ -component and lower row the  $E_x$ -component.

As seen in Fig.3, solderjet technology produced almost no influence on the output field; and consequently, almost no influence on the laser beam output emission.

## 5. Conclusions and outlook

The mechanico-optical simulations used to analyze stress-induced effects on laser ignition devices packaged by the solderjet bumping technique showed almost no consequences on the laser output beam. Moreover, the use of four 760  $\mu\text{m}$  diameter SAC305 bumps granted a join strength of  $\sim 100$  N and a good thermal contact.

## 6. Acknowledgments

The authors acknowledge partial support from the European Union's Horizon 2020 Research and Innovation Programme under grant agreement No 691688.

## 7. References

- [1] E. Beckert, T. Oppert, G. Azdasht, E. Zakei, T. Burkhardt, M. Hornaff, A. Kamm, I. Scheidig, R. Eberhardt, A. Tünnermann, F. Buchmann, "Solder jetting—a versatile packaging and assembly technology for hybrid photonics and optoelectronic systems," in Proceedings of IMAPS 42nd Int. Symp. on Microelectronics, California, (2009) pp. 406.
- [2] P. Ribes-Pleguezuelo, A. Moral, M. Gilaberte, P. Rodríguez, G. Rodríguez, M. Laudisio, M. Galan, M. Hornaff, E. Beckert, R. Eberhardt, A. Tünnermann, "Assembly processes comparison for a miniaturized laser used for the Exomars European Space Agency mission", Optical Engineering, SPIE, DOI: 10.1117/1.OE.55.11.116107, USA (2016).
- [3] G. Salamu, A. Ionescu, C. Brandus, O. Grigore, N. Pavel, T. Dascalu, "Generation of High-Peak Power 532-nm Green Pulses from Composite, All-Ceramics, Passively Q-switched Nd:YAG/Cr4+:YAG Laser", in Proceedings of SPIE Vol. 8882, 888206, Tenth Conference on Optics: Micro- to Nanophotonics III, Romania (2012).
- [4] P. Ribes-Pleguezuelo, S. Zhang, E. Beckert, R. Eberhardt, F. Wyrowski, A. Tünnermann, are submitting a Optics Express journal article to be called Method to simulate and analyse induced stresses for laser crystal packaging technologies.
- [5] Q. Lü, U. Wittrock, S. Dong, "Photoelastic effects in Nd:YAG rod and slab lasers", Optics & Laser Technology 27 No 2, Elsevier, Germany (1995).